

Class II selective Histone deacetylase inhibitors (HDACi) as therapeutics for Type 2 Diabetic Retinopathy: An in silico approach

Devkinandan Sharma*, Priyanka Mishra, Dr. Archana tiwari

School of Biotechnology - UTD, Rajiv Gandhi Proudyogiki Vishwavidyalaya, Bhopal, Madhya Pradesh - 462033 India

DOI: 10.36347/sajb.2019.v07i07.006

| Received: 20.08.2019 | Accepted: 27.08.2019 | Published: 30.08.2019

*Corresponding author: Devkinandan Sharma

Abstract

Original Research Article

From chronically diabetic retinopathy upsurge the augur of diabetes can lead to irreversible vision loss. In the present chronological time, no cure in early-stage is possible in case of Diabetic Retinopathy (DR). Decreased the level of BDNF gene association between type II diabetes and class II Histone deacetylase (HDACs) as both increases; Histone deacetylases (HDACs) regulate epigenetic gene expression programs by modulating chromatin architecture and are required for neuronal development. Dysregulation of HDACs and aberrant chromatin acetylation homeostasis have been implicated in various diseases ranging from cancer to neurodegenerative disorders, for instance, DR. Class- II selective Histone deacetylase inhibitors (HDACi) have implications in increasing synaptic plasticity, decreasing angiogenesis, triggering neuroprotective signaling and positively suppress abnormal development of blood vessels. HDACi also shows promise as therapeutics for neurodegenerative. Here, we propose in-silico research that-there is a strong rationale for early treatment of diabetic retinopathy with aim and objective of this erudite research is insilico approach to investigate the binding affinity of Class- II selective Histone Deacetylase towards BDNF-TrkB pathway. The docking was done using "AutoDock vina and Swissdock" and visualized it through "UCSF chimera & Discovery Studio 2017 R2 Client". Protein-protein analysis and visualization of docking simulation results were done using "HEX Server". Molecular docking results of every Class- II Histone Deacetylase Inhibitors towards Trk-B receptor have negative binding energy, whereas E-total and E-shape value with greater than -7 and RMS values having negative $-0.5 \leq 1$. This research concludes that our findings implicate class II selective HDAC inhibitors in triggering neuroprotective signaling that can be increased expression of BDNF gene and indicate that class II selective HDAC inhibitors are an approach towards personalized medicine for early Diabetic Retinopathy.

Keywords: Diabetic Retinopathy (DR), Brain-derived neurotrophic factor (BDNF), Molecular docking, class -II HDACi (Histone Deacetylase Inhibitor).

Copyright © 2019: This is an open-access article distributed under the terms of the Creative Commons Attribution license which permits unrestricted use, distribution, and reproduction in any medium for non-commercial use (NonCommercial, or CC-BY-NC) provided the original author and source are credited

INTRODUCTION

Type II Diabetic Retinopathy (T2DR), which is a micro-vascular complicacy, leads to cause acquired blindness in both young and adults. Many molecular and biochemical regulation have been found to be involved in its pathogenesis. During slowly progressive disease, different early and late histopathological alterations occur which includes venous bleeding, cotton wool spots, micro-aneurysms, intraretinal microvascular abnormalities, and haemorrhages. If not treated, it leads to more advanced stages, which concludes the development of new fragile blood vessels on the posterior surface of the vitreous along with the retina which might result in the detachment of the retina, finally leads to blindness [1].

Being a neuronal tissue of the eye, retina produces different neurotrophic factors, which comprises brain-derived neurotrophic factor (BDNF), nerve growth factor (NGF), neurotrophin-3, and neurotrophin-4. BDNF which is known to be responsible for the maintenance and regulation of neuronal cells is mainly produced by neurons and glial cells in the retina of the eye [2]. Downstream signalling pathways of BDNF depend on two distinct receptors which include p75 neurotrophin receptor and tropomyosin-related kinase receptor B (TrkB). Dysregulation of such neurotrophic factors leads to cause pathologic angiogenesis and Neuro-degeneration in different diseases including proliferative diabetic retinopathy (PDR) [3]. The levels of BDNF decreased in the serum of diabetic patients and in diabetic animals, which has been reported in various studies, which is correspond

with insulin resistance and reduced level of glucose metabolism [4].

Decreased the level of *BDNF* gene association between type II diabetes and class II Histone deacetylase (HDACs) as both increases; Histone deacetylases (HDACs) regulate epigenetic gene expression programs by modulating chromatin architecture and are required for neuronal development. Dysregulation of HDACs and aberrant chromatin acetylation homeostasis have been implicated in various diseases ranging from cancer to neurodegenerative disorders, for instance, DR [5].

The process of eradication of functional acetyl groups from histone's lysine residues is carried out by the enzyme Histone deacetylases (HDACs). At present, there are 18 HDAC enzymes found in humans, which deacetylate acetyl-lysine residue by applying either NAD^+ - or zinc-dependent mechanisms. In humans, 18 HDAC enzymes are categorized into four classes designated as Class I Rpd3-like proteins which comprise of HDAC3, HDAC2, HDAC1, and HDAC8; Class II Hda1-like proteins comprise of HDAC6, HDAC5, HDAC4, HDAC10, HDAC9, and HDAC7; Class III Sir2-like proteins consist of SIRT3, SIRT2, SIRT1, SIRT7, SIRT6, SIRT5, and SIRT4; and the Class IV protein contain HDAC11. From ϵ -amino lysines, HDACs evacuate acetyl groups, which not only modify the transcription process but also promote governance alternation of posttranslational modifications of lysine residue which comprise of ubiquitination, sumoylation, and methylation [6].

At present, a number of compounds have been flourished and distinguished which inhibit HDAC activities. They are described in causing of cells differentiation or apoptosis and cells growth arrest. Research showing that an enormous number of human diseases tightly correlated with epigenetic abnormalities, implementing class – II selective HDAC inhibitors might rationale exploit in epigenetic-based therapies in case of T2DR. Class- II selective Histone deacetylase inhibitors (HDACi) have implications in increasing synaptic plasticity, decreasing angiogenesis, triggering neuroprotective signaling and positively suppress abnormal development of blood vessels. Class- II selective HDACi also shows promise as therapeutics for neurodegenerative [7].

Significantly, no treatment is approved for early phases of diabetic retinopathy [8]. If inactivation of the BDNF- TrkB pathway happens, it leads us to early retinal damage of diabetic subjects. Hence, this aimed us- at the identification of agonist for BDNF- TrkB pathway by Class- II Histone Deacetylase Inhibitors and BDNF- TrkB pathway interaction that might be biomarkers and pharmacological targets for personalized medicine and treatment of early diabetic retinopathy. It set out of study vision based on Class- II selective

Histone Deacetylase Inhibitors that target BDNF-TrkB signalling presently used as anti-cancer drug have been able to suppressed neuro-degeneration by increased expression of Brain-derived neurotrophic factor (*BDNF*) such as Trichostatin A (TSA), Suberoylanilide Hydroxamic Acid (*SAHA*), Panobinostat (*LBH589*), Belinostat (*PXD101*).

MATERIAL AND METHODS

Collecting the Homo sapiens Class II HDAC sequences, protein and its 3D structure

Collecting of Homo sapiens Class II HDACi sequences was downloaded from the ZINC database at site (<https://zinc.docking.org>). The Homo sapiens Trk-b receptor protein 3D crystal structure was downloaded from the PDB structural database at site (<http://www.rcsb.org/pdb>).

Ramachandran Plot Analysis

Ramachandran plot analysis was done by using Ramphge is free online available tool at site (<http://mordred.bioc.cam.ac.uk/~rapper/rampage.php>).

Preparation of class II HDAC Homo sapiens inhibitor file

Class II Homo sapiens inhibitor such as Trichostatin A (TSA), suberoylanilide hydroxamic acid (*SAHA*), panobinostat (*LBH589*), Belinostat (*PXD101*), mol file were loaded with MarvinSketch software was downloading from online at site (<https://chemaxon.com/products/marvin>) and explicit hydrogen to each ligand file. Ligands file were saved in pdb 3D structure format.

Analysis and visualization of Molecular docking results

The docking was done using “AutoDock vina and Swissdock” and visualized it through “UCSF chimera & Discovery Studio 2017 R2 Client”. Protein-protein analysis and visualization of docking simulation results were done using “HEX Server”.

RESULTS AND DISCUSSION

Ramachandran plot analysis of TrKb and BDNF protein

Table-1 and Figure 1 & 2 showed that The result of ramchandran plot of *Tropomyosin receptor kinase B (TrkB)* and Brain-derived neurotrophic factor (BDNF) protein are PDB ID: 4AT5 AND 1B8M consecutively. Ramachandran Plot is used as tool to validate the modeled protein structure based on the ϕ (phi), ψ (psi) and ω (omega) angles. This validation determines the quality of the protein structure, good quality in turn reflects in efficient and accurate docking results. The denser number of residues in favoured region (>90%) is the measure of good quality of a model [9].

Ramachandran plot of BDNF (1B8M) protein by Rampage

In this present observation (Fig-1) illustrates that in BDNF protein total 206 amino acid residues present in

favourable region which contain 94.5%, 8(3.7%) were in allowed region and 4(1.8%) were in outlier region.

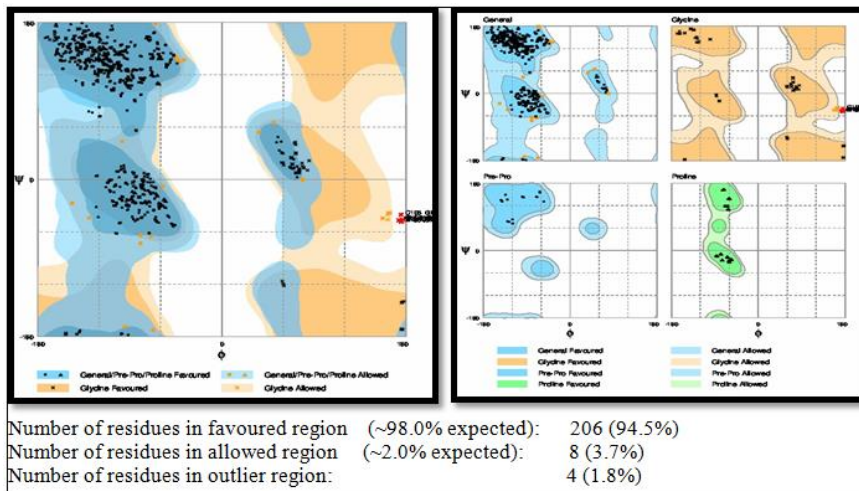


Fig-1: Rampage of BDNF (1B8M) protein

Ramachandran plot of TrKB (4at5) receptor protein

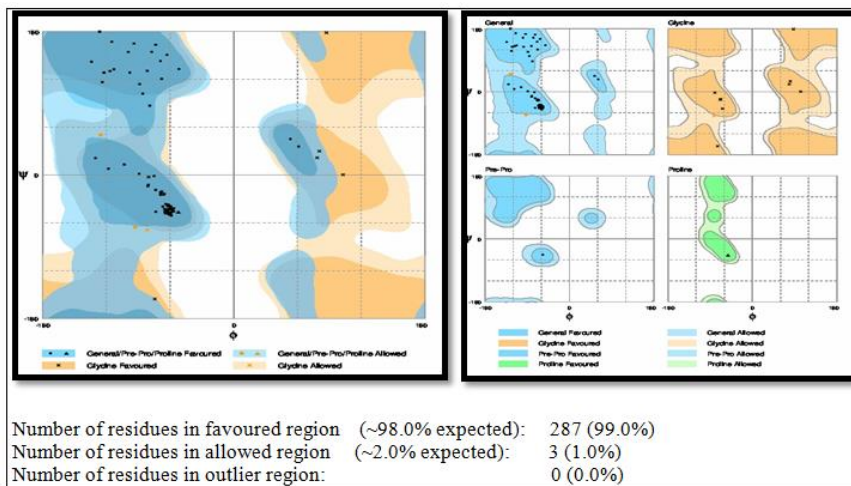


Fig-2: Rampage of TrKB protein

Fig-2 demonstrated that in TrKB protein total 287 amino acid residues present in favourable region

which contains 99.0%, 3(1.0%) were in allowed region and 0(0.0%) were in outlier region.

Table-1: Rampage of protein

Protein	Favoured Region	Allowed Region	Outlier Region
BDNF	206 (94.5%)	8 (3.7%)	4 (1.8%)
4AT5	287 (99.0%)	3 (1.0%)	0 (0.0%)

Table-1 illustrates RAMPAGE of protein Results include BDNF protein total 206 amino acid residues present in favourable region which contain 94.5%, 8(3.7%) were in allowed region and 4(1.8%)were in outlier region. TrKB protein total 287 amino acid residues present in favourable region which contain

99.0%, 3(1.0%) were in allowed region and 0(0.0%) were in outlier region. The denser number of residues in favoured region (>90%) is the measure of good quality of a model [9].

Molecular Docking

Protein-ligand docking process was done by using Swiss dock and Autodock vina. Results were stored in PDB format. Ligand conformation that has the lowest binding energy was chosen to determine protein-ligand conformation from docking result. The selected protein-ligand complex was having a low binding energy value greater than -5 for further analysis. Visualization of 3D complex interactions with ligands protein was done through the rendering process. After going through the process, the 3D structure of the protein can be illustrated through maps on the navigation of the surface and software menu. Then, the interacting ligand, cofactor, and the enzyme amino acid residues could be displayed. Interaction of amino acid residues in protein with ligands can be viewed by using the features of chimaera. Initially, the ligand was selected using the browser menu. Protein-ligand complex energy was minimized with the chimera Minimize menu and then clicks the Interaction menu. After that, an analysis of the interactions that occurred between amino acid residues in protein with ligand inhibitor was conducted.

Molecular docking process was selected class II HDACi with Tropomyosin receptor kinase B (TrKB). Docking process takes 18-50 hours, depending on the computer processor specifications. The selected best ligands are Trichostatin A (TSA), Suberoylanilide hydroxamic acid (SAHA), Panobinostat (LBH589), Belinostat (PXD101). The binding free energy ($\Delta G_{binding}$) of the best ligand with HDAC enzymes is presented in Table-3.

After getting the value of ΔG -binding molecular docking results, the next step is to analyze the interaction between Tropomyosin receptor kinase B (TrKB) receptor protein with the selected class II HDAC ligand inhibitor. From the results of molecular docking database, the selected file-browser menu would determine the ligand interactions. After the minimization of energy, visualization of the interaction between the protein and the ligand was obtained *is* presented in SWISS DOCK and AUTODOCK VINA result Figure-2.

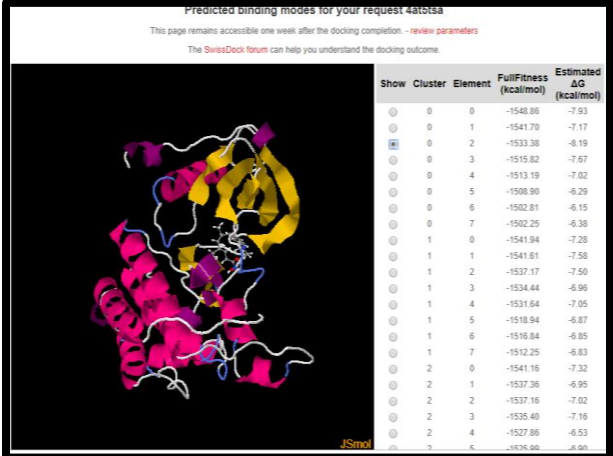
In Figure-3, the interaction was formed between 4AT5 and TSA. Results were analyzed using molecular docking of swiss dock software. Visualization of 3D complex interactions with ligands enzyme was done through chimera software. After going through the automatic online process of swiss dock software, results are obtained on the navigation of surface and compute menu in Swiss Dock software. Docking results were stored in pdbqt format. Then, the interacting ligand, binding energy, and the protein amino acid residues could be displayed is showing in Figure-3, that after interaction of 4AT5 with TSA, delta-G value obtain were -7.93 and full fitness score was -1548.86.

In Figure-4, the interaction was formed between 4AT5 and SAHA. Results were analyzed using

molecular docking of swiss dock software. Visualization of 3D complex interactions with ligands enzyme was done through chimera software. After going through the automatic online process of swiss dock software, results are obtained on the navigation of surface and compute menu in Swiss Dock software. Docking results were stored in pdbqt format. Then, the interacting ligand, binding energy, and the protein amino acid residues could be displayed is showing in Figure-5, that after interaction of 4AT5 with SAHA, delta-G value obtain were -7.55 and full fitness score was -1591.85.

In Figure-5, the interaction was formed between 4AT5 and PXD101. Results were analyzed using molecular docking of swiss dock software. Visualization of 3D complex interactions with ligands enzyme was done through chimera software. After going through the automatic online process of swiss dock software, results are obtained on the navigation of surface and compute menu in Swiss Dock software. Docking results were stored in pdbqt format. Then, the interacting ligand, binding energy, and the protein amino acid residues could be displayed is showing in Figure-6, that after interaction of 4AT5 with PXD101, delta-G value obtain were -8.55 and full fitness score was -1591.06.

In Figure-6, the interaction was formed between 4AT5 and LBH589. Results were analyzed using molecular docking of Swiss dock software. Visualization of 3D complex interactions with ligands enzyme was done through chimera software. After going through the automatic online process of Swiss dock software, results are obtained on the navigation of surface and compute menu in Swiss Dock software. Docking results were stored in pdbqt format. Then, the interacting ligand, binding energy, and the protein amino acid residues could be displayed is showing in Figure-7, that after interaction of 4AT5 with LBH589, delta-G value obtain were -8.42 which was greater negative value than -5 and full fitness score was -1556.92.



Show	Cluster	Element	FullFitness (kcal/mol)	Estimated ΔG (kcal/mol)
<input type="radio"/>	0	0	-1548.86	-7.93
<input type="radio"/>	0	1	-1541.70	-7.17
<input checked="" type="radio"/>	0	2	-1533.38	-8.19
<input type="radio"/>	0	3	-1515.82	-7.67
<input type="radio"/>	0	4	-1513.19	-7.02
<input type="radio"/>	0	5	-1508.90	-6.29
<input type="radio"/>	0	6	-1502.81	-6.15
<input type="radio"/>	0	7	-1502.25	-6.38
<input type="radio"/>	1	0	-1541.94	-7.28
<input type="radio"/>	1	1	-1541.61	-7.58
<input type="radio"/>	1	2	-1537.17	-7.50
<input type="radio"/>	1	3	-1534.44	-6.96
<input type="radio"/>	1	4	-1531.64	-7.05
<input type="radio"/>	1	5	-1518.94	-6.87
<input type="radio"/>	1	6	-1516.84	-6.85
<input type="radio"/>	1	7	-1512.25	-6.83
<input type="radio"/>	2	0	-1541.16	-7.32
<input type="radio"/>	2	1	-1537.36	-6.95
<input type="radio"/>	2	2	-1537.16	-7.02
<input type="radio"/>	2	3	-1535.40	-7.16
<input type="radio"/>	2	4	-1527.86	-6.53
<input type="radio"/>	3	5	-1676.00	-8.00

Fig-3: Interaction with 4AT5 and TSA

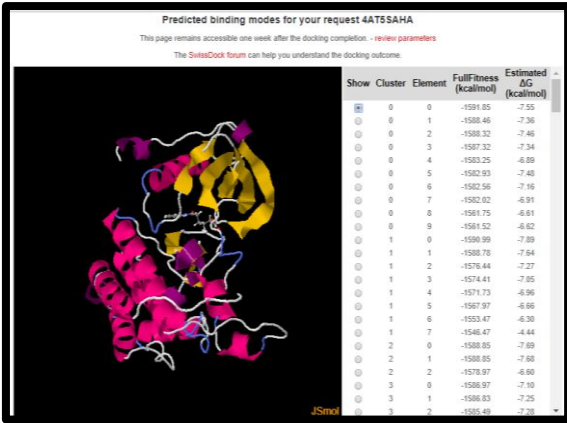


Fig-4: Interaction with 4AT5 and SAHA

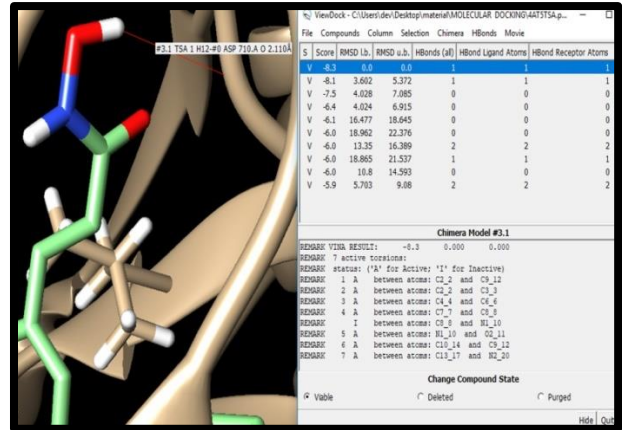


Fig-7: Interaction with 4AT5 and TSA

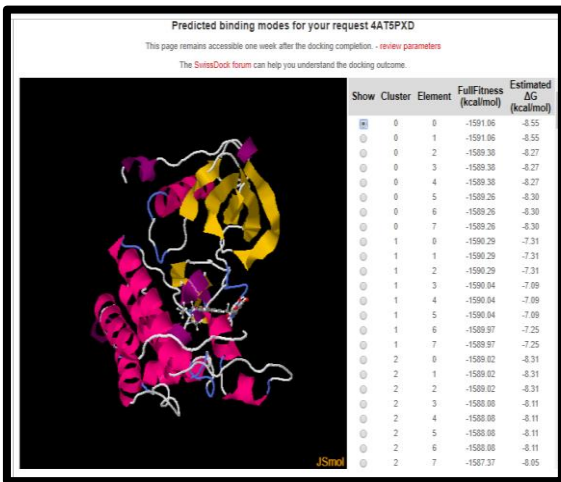


Fig-5: Interaction with 4AT5 and PXD101

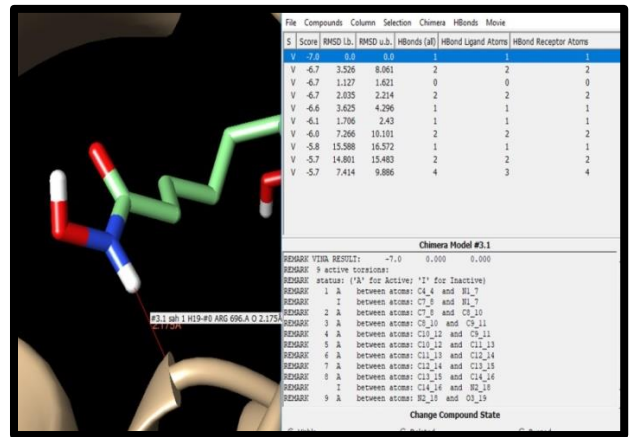


Fig-8: Interaction with 4AT5 and SAHA

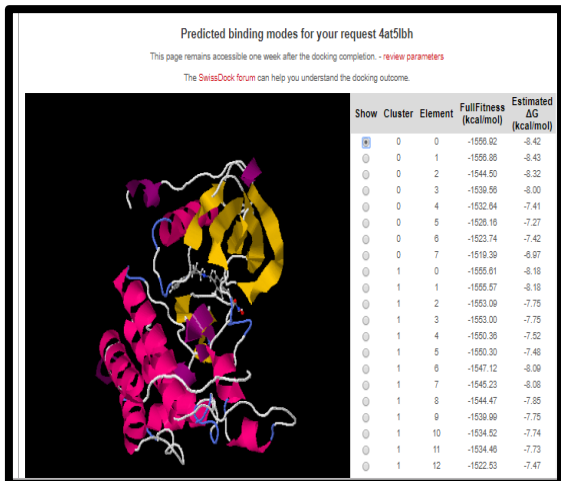


Fig-6: Interaction with 4AT5 and LBH

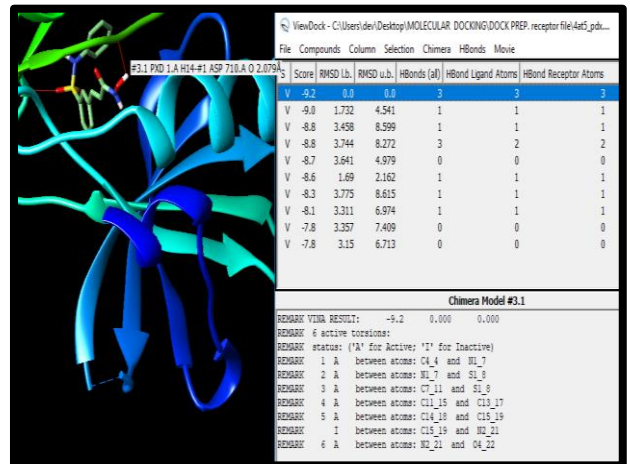


Fig-9: Interaction with 4AT5 and PXD101

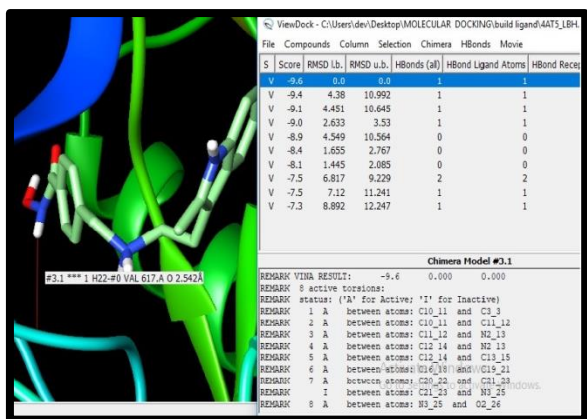


Fig-10: Interaction with 4AT5 and LBH

In Figure-7, the interaction was formed between 4AT5 and TSA. Results were analyzed using molecular auto docking process of chimera software. Visualization of 3D complex interactions with ligands protein was done through chimera software. After the interaction of TSA interaction with TrKB, the figure shows that 9 conformant results of docking Autodock Vina. Crystal structure of 4AT5 show higher binding affinity with TSA was -8.3 and hydrogen bond shows was ASP-710.

In Figure-8, the interaction was formed between 4AT5 and SAHA. Results were analyzed using molecular auto docking process of chimera software. Visualization of 3D complex interactions with ligands protein was done through chimera software. After the interaction of Suberanilo hydroxamic (SAHA) interaction with TrKB, the figure shows that 9 conformant results of docking Autodock Vina. Crystal structure of 4AT5 show higher binding affinity with SAHA was -6.1 and hydrogen bond shows was ASP-710.

In Figure-9, the interaction was formed between 4AT5 and PXD101. Results were analyzed using molecular auto docking process of chimera software. Visualization of 3D complex interactions with ligands protein was done through chimera software. After PXD interaction with TrKB, shows that 6 conformant results of docking Autodock Vina. Crystal structure of 4AT5 show higher binding affinity with VPA was -9.2 and hydrogen bond shows was ASP 710.

In Figure-10, the interaction was formed between 4AT5 and LBH589. Results were analyzed using the molecular auto-docking process of chimera software. Visualization of 3D complex interactions with ligands protein was done through chimera software. After Panobinostat (LBH589) interaction with TrKB, shows that 8 conformant results of docking Autodock Vina. Crystal structure of 4AT5 show higher binding affinity with SAHA was -9.6 and hydrogen bond shows was VAL 617.

Table-3: The binding free energy ($\Delta G_{binding}$) of the selected class II HDACi with TrKB receptor protein

Ligand Name	Zinc ID	Receptor TrKB-4AT5	
		SWISS DOCK	AUTODOCK
SAHA	1543873	-7.55	-7.0
LBH589	22010649	-8.42	-9.6
PXD101	3820616	-8.65	-9.2
TSA	5298929	-7.93	-8.3

Note: The number in bold is the lowest free energy value

Table-3 Illustrated result from docking using Swiss dock and Autodock vina include, interaction of TrKB (4AT5)- LBH589, TrKB (4AT5)-PXD101, TrKB (4AT5) -TSA, TrKB (4AT5)- SAHA were binding energy -8.42,-8.65,-7.93 and -7.55 or -9.6,-9.2, -8.3, and -7.0, respectively.

Which conclude that every interaction was greater negative value than -5 is the measure of good docking results between class II HDACi ligand and TrKB protein. Earlier studies of a molecule determine the interaction data of cyclic peptide inhibitor with the extracellular domain of TrKB receptor [10]. Computational Design of TrKB Peptide inhibitors and their biological effects on Ovarian Cancer Cell lines include Interaction of TrKB- PEP5 show binding affinity was -7.0 and TrKB - Cyclotraxin B was greater negative value than -5 [11]. In this report, the best interaction of class II HDACi and TrKB shows binding affinity having greater negative value than -5 therefore it had been predicted that II HDACi can activate TrKB receptor, thus it would be helpful in case of T2DR.

VISUALIZATION

Visualization of the interaction between the receptor protein TrKB with TSA ligand showed three conventional hydrogen bonding interaction with two residues of the TrKB protein active sites (Asp710, and Asp640) (Figure 5.2.9). There is carbon-hydrogen bonding interaction to oxygen with the side-chain residue of Gly 639.

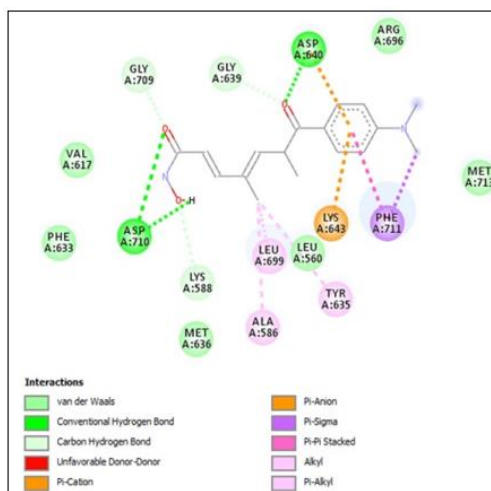


Figure 5.2.9: Visualization TrKB protein and TSA ligand

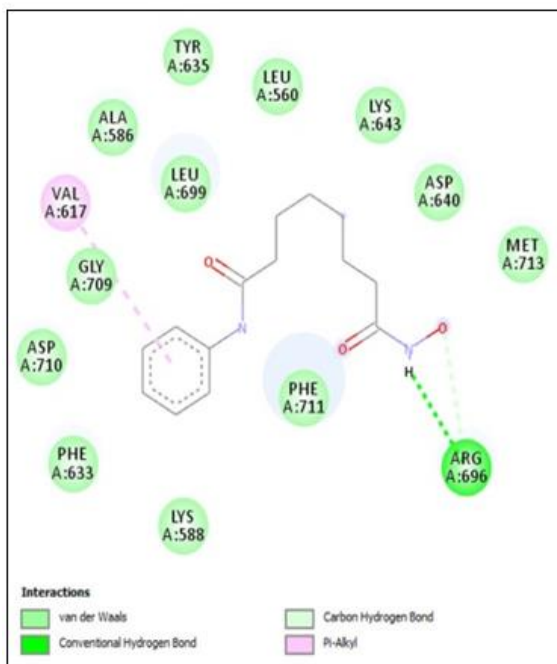


Figure 5.2.10: Visualization TrKB protein and SAHA ligand

Next on the Visualization of the interaction between the receptor protein TrKB with SAHA ligand showed one conventional and one carbon-hydrogen bonding interaction with one residue of the TrKB protein active sites (Arg696) (In figure 5.2.10).

In figure 5.2.11, Visualization of the interaction between the receptor protein TrKB with PXD101 ligand showed four conventional hydrogen bonding interaction with three residues of the TrKB protein active sites (Asp710, Asp640 and Lys 643). One hydrogen bonding interaction between the H bonded to nitrogen with the side-chain residue of Asp640 and other three bonded to oxygen atoms.

In figure 5.2.12, visualization of the interaction between the receptor protein TrKB with LBH589 ligand showed one conventional hydrogen bonding interaction between the H bonded to nitrogen with the side-chain residue of Val617 which is the residue of the TrKB protein active sites.

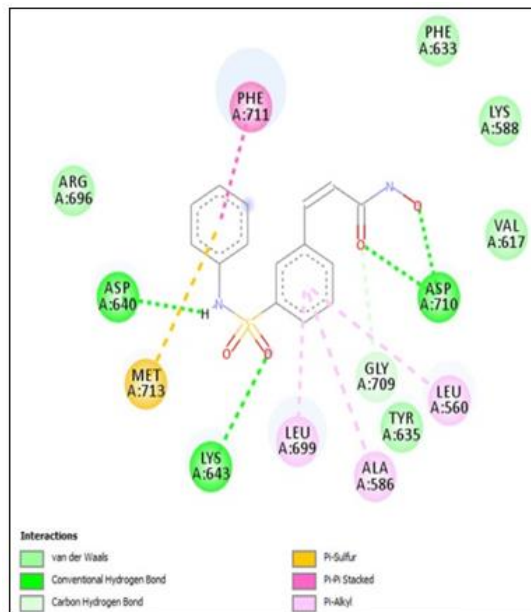


Figure 5.2.11: Visualization TrKB protein and PXD101 ligand

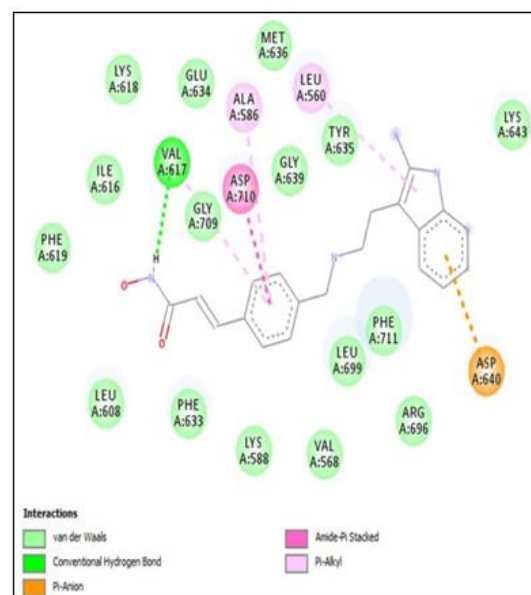


Figure 5.2.12: Visualization TrKB protein and LBH589 ligand

Hex server

Top three Interaction result of docked TrKB (4AT5) and HDACi with BDNF (1B8M)

Table-4: Top three Interaction result of docked TrKB (4AT5) and Class II HDACi with BDNF (1B8M)

Name List	E-total	E-shape	RMS
Trichostatin A (TSA)	-714.35	-714.35	-1
LBH589	-730.32	-730.32	-1
PXD101	-713.93	-713.93	-1

Interaction of docked TrKB (4AT5) and TSA with BDNF (1B8M)

Hex server is communally available to users of the protein-protein interactions. Hex Server is the first

Fourier transform (FFT)-based protein docking server to be powered by graphics processors. Interaction of docked TrKB (4AT5) and TSA is a direct binding BDNF protein.

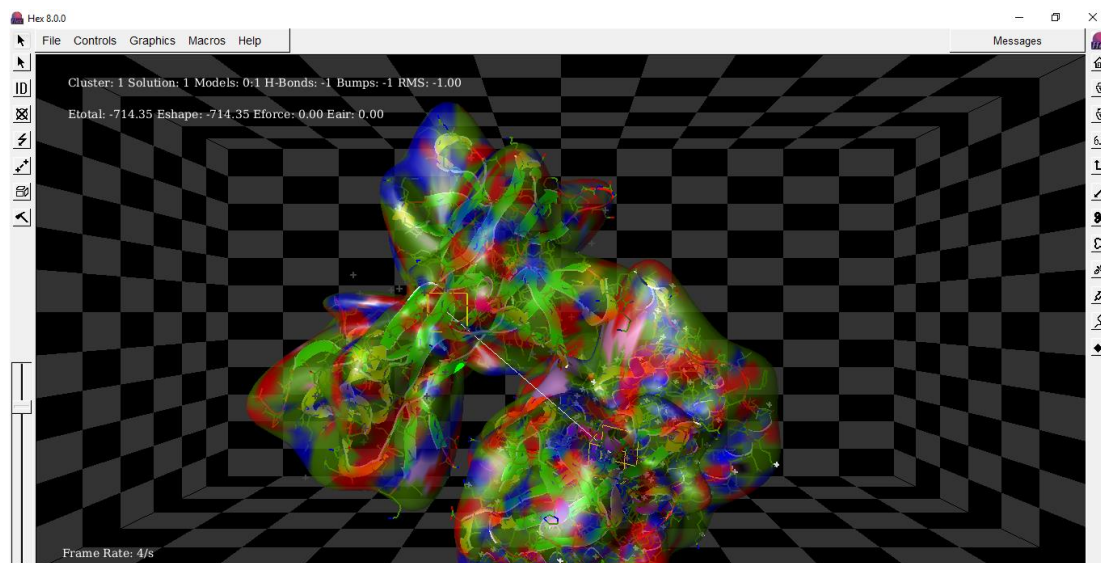


Fig-11: Interaction result of docked TrKB (4AT5) and TSA with BDNF (1B8M)

The result obtained from (Fig-11) showed that interaction of docked TrKB (4AT5) and TSA with BDNF (1B8M). When they bind to each other through

the disulfide bond and average RMS value was -1 and maximum E-total and E-shape value was -714.35 and -714.35.

Interaction of docked TrKB (4AT5) and LBH589 with BDNF (1B8M)

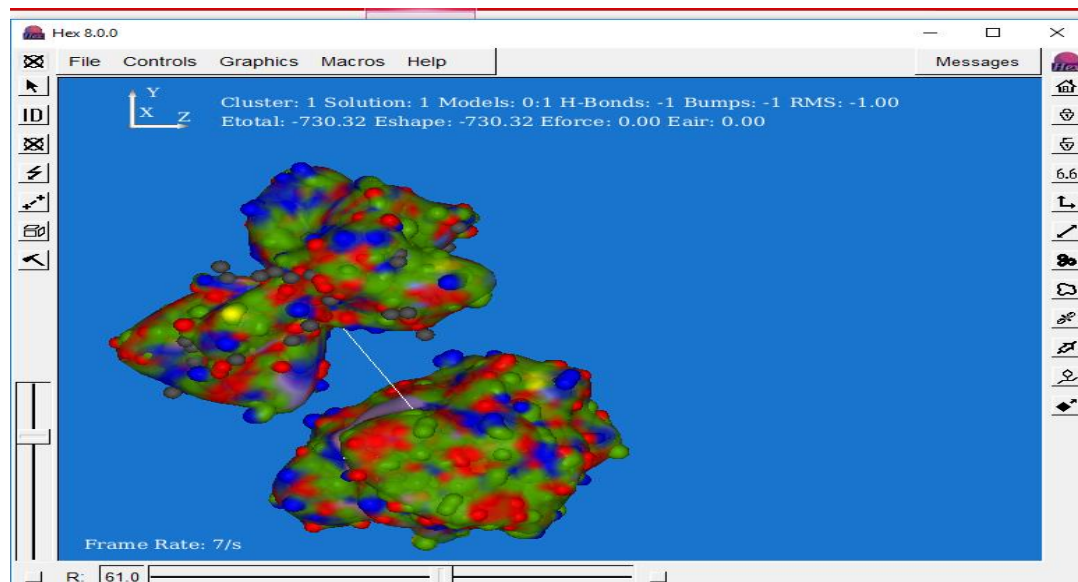
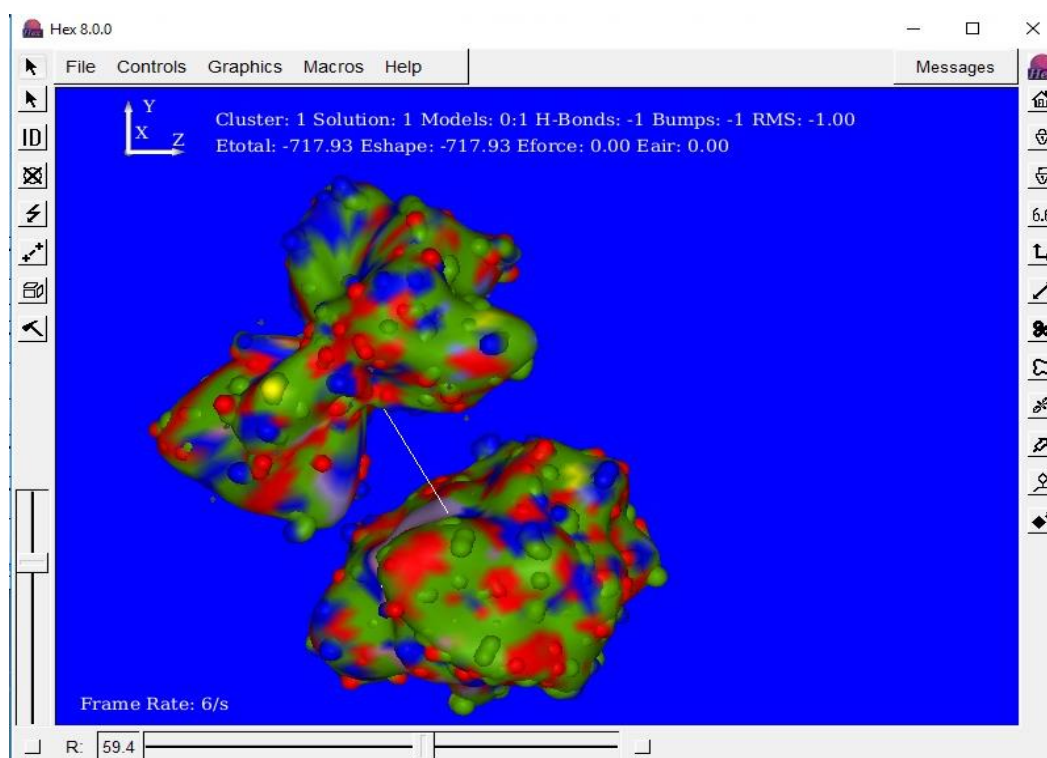


Fig-12: Interaction result of docked TrKB (4AT5) and LBH 589 with BDNF (1B8M)

The result obtained from (Fig-12) showed that interaction of docked TrKB (4AT5) and LBH with BDNF (1B8M). When they bind to each other through

the disulfide bond and average RMS value was -1 and maximum E-total and E-shape value was -730.32 and -730.32.

Interaction of docked TrKB (4AT5) and PDX101 with BDNF (1B8M)**Fig-13: Interaction result of docked TrKB (4AT5) and PDX101 with BDNF (1B8M)**

The result obtained from (Fig-13) showed that interaction of docked TrKB (4AT5) and PDX101 with BDNF (1B8M). When they bind to each other through the disulfide bond and average RMS value was -1 and maximum E-total and E-shape value was -713.93 and -717.93.

Result obtained from Fig 11-13 and Table-4 showed that interaction results of docked TrKB (4AT5) -TSA, TrKB (4AT5)- LBH589, TrKB (4AT5)-PDX101 with BDNF (1B8M).TrKB (4AT5) - LBH589 shows the best interaction when they bind to each other through the disulfide bond and average RMS value was -1 and maximum E-total and E-shape value were -730.32 and -730.32. In the past literature reviewed prediction of protein-ligand interaction for snake venom protein was studied and e-value was obtained -111.73. Molecular Docking Studies of anti-HIV drug BMS-488043 the HEX docking results reveal that the e-value of Analog 8 (-263.29) is better as compared to that of the original drug. Docking results between the Iodo derivative of pyrrole with few selected receptors are best with the highest negative value 3MNW (energy value -265.9) was selected [12]. In this present study, the result obtains from docked Class-II selective Histone Deacetylase Inhibitors &TrKB receptor with BDNF have negative binding energy whereas E-total and E-shape value was greater than -7 and RMS value was negative $-0.5 \leq 1$. It may be predicted that class II HDAC Homosapiens can activate BDNF- TrKB pathway. Hence Role of Histone Deacetylase inhibitors in BDNF-TrKB signaling for

epigenetic management of Diabetic Retinopathy: *In silico* analysis an approach towards personalized medicine for Type II Diabetic Retinopathy.

CONCLUSIONS

Recent progress in the understanding of T2DR pathogenesis has led to significant advances in available pharmacotherapy; however, a cure for T2DR has yet to be realized. In the context of the literature review, molecular docking of Class-II selective Histone Deacetylase Inhibitors &TrKB receptor with BDNF to trigger neuroprotective signaling in Type II Diabetic Retinopathy has not been studied so far. Therefore, there is a need to design molecular compound which can control the acetylation pattern and alternately controls T2DR. The present research focused on the role of Histone Deacetylase inhibitors in BDNF-TrKB signaling for epigenetic management of Diabetic Retinopathy for the pathogenesis of T2DR. Regarding for this, gathering of Homo sapiens Class II HDACi ZINC IDs has been downloaded from the ZINC database and the Homo sapiens TrKB, receptor (PDB ID 4AT5) and BDNF (PDB ID: 1B8M) has been downloaded from the PDB structural database. The docking was done using "AutoDock vina and Swiss dock" and visualized it through "UCSF chimera & Discovery Studio 2017 R2 Client". Protein-protein analysis and visualization of docking simulation results were done using HEX Server.

Molecular docking results of every Class- II Histone Deacetylase Inhibitors towards Trk-B receptor have negative binding energy, whereas-total and E-shape value with greater than -7 and RMS values having negative $-0.5 \leq 1$. Hence, it can be activated BDNF-TrkB pathway may be helpful for regulating the regulation of BDNF gene expression which in turn would be helpful in case of T2DR by regulating retinal cell survival and cell differentiation.

This study concludes that our findings implicate class II selective HDAC inhibitors in triggering neuroprotective signaling that can be increased expression of BDNF gene and indicate that class II selective HDAC inhibitors are an approach towards personalized medicine for Diabetic Retinopathy.

REFERENCES

1. Antonetti DA, Barber AJ, Bronson SK, Freeman WM, Gardner TW, Jefferson LS, Kester M, Kimball SR, Krady JK, LaNoue KF, Norbury CC. Diabetic retinopathy: seeing beyond glucose-induced microvascular disease. *Diabetes*. 2006 Sep 1;55(9):2401-11.
2. Seki M, Tanaka T, Sakai Y, Fukuchi T, Abe H, Nawa H, Takei N. Müller cells as a source of brain-derived neurotrophic factor in the retina: noradrenaline upregulates brain-derived neurotrophic factor levels in cultured rat Müller cells. *Neurochemical research*. 2005 Sep 1;30(9):1163-70.
3. Suchting S, Bicknell R, Eichmann A. Neuronal clues to vascular guidance. *Experimental cell research*. 2006 Mar 10;312(5):668-675.
4. Yamanaka M, Itakura Y, Ono-Kishino M, Tsuchida A, Nakagawa T, Taiji M. Intermittent administration of brain-derived neurotrophic factor (BDNF) ameliorates glucose metabolism and prevents pancreatic exhaustion in diabetic mice. *Journal of bioscience and bioengineering*. 2008 Apr 1;105(4):395-402.
5. Ganai SA, Abdullah E, Rashid R, Altaf M. Combinatorial in silico strategy towards identifying potential hotspots during inhibition of structurally identical HDAC1 and HDAC2 enzymes for effective chemotherapy against neurological disorders. *Frontiers in molecular neuroscience*. 2017 Nov 9;10:357.
6. Kowluru RA. Diabetic retinopathy, metabolic memory and epigenetic modifications. *Vision research*. 2017 Oct 1;139:30-38.
7. Koppel I, Timmusk T. Differential regulation of Bdnf expression in cortical neurons by class-selective histone deacetylase inhibitors. *Neuropharmacology*. 2013 Dec 1;75:106-115.
8. Platania CB, Maisto R, Trotta MC, D'Amico M, Rossi S, Gesualdo C, D'Amico G, Balta C, Herman H, Hermenean A, Ferraraccio F. Retinal and circulating mi RNA expression patterns in diabetic retinopathy: An in silico and in vivo approach. *British journal of pharmacology*. 2019 Jul 1; 176(13):2179-2194.
9. Bilal S, Iqbal H, Anjum F, Mir A. Prediction of 3D structure of P2RY5 gene and its mutants via comparative homology modelling. *Journal of Computational Biology and Bioinformatics Research*. 2009 Nov 30;1(1):11-16.
10. Chitranshi N, Gupta V, Dheer Y, Gupta V, Vander Wall R, Graham S. Molecular determinants and interaction data of cyclic peptide inhibitor with the extracellular domain of TrkB receptor. *Data in brief*. 2016 Mar 1;6:776-82.
11. Poorebrahim M, Najafi S, Rahimi H, Karimipour M, Gheibi N. Computational design of trkb peptide inhibitors and their biological effects on ovarian cancer cell lines. *International Journal of Peptide Research and Therapeutics*. 2016 Sep 1;22(3):289-99.
12. Patel UH, Barot RA, Patel BD, Shah DA, Modh RD. Docking studies of pyrrole derivatives using Hex. *International Journal of Environmental Sciences*. 2012;2(3):1765-70.